applied sciences

MDPI

Article

An Adaptive and Bounded Controller for Formation Control of Multi-Agent Systems with Communication Break

Zhigang Xiong, Zhong Liu, Yasong Luo * and Jiawei Xia

College of Weapon Engineering, Naval University of Engineering, Wuhan 430034, China; xiongzgzm2@163.com (Z.X.); lzhong@163.com (Z.L.); wilson0078@163.com (J.X.)
* Correspondence: yoursbaggio@163.com

Abstract: AbstractAiming at maneuvering, input saturation, and communication interference in the controller design for formation control multi-agent systems, a novel nonlinear bounded controller is proposed. Based on coordinates transformation, reference information is processed, and nonlinear effects of maneuvering are analyzed. Then a nonlinear controller is established with graph theory, consensus algorithm, and Lyapunov method, which guarantee the stability of the controller. For input saturation avoidance, adaptive parameters are put forward with the Lyapunov function. Considering the communication breaks, various conditions of the sensing graph are discussed for stable formation control, and a dynamic programming regulator is proposed for unknown position reference needed for formation keeping. Comparison with the traditional consensus method is provided in numerical simulation to verify the stability and feasibility of the proposed strategy.

Keywords: formation control; input saturation; Lyapunov function; multi-agent systems

check for updates

Citation: Xiong, Z.; Liu, Z.; Luo, Y.; Xia, J. An Adaptive and Bounded Controller for Formation Control of Multi-Agent Systems with Communication Break. *Appl. Sci.* **2022**, *12*, 5602. https://doi.org/10.3390/app12115602

Academic Editor: Dario Richiedei

Received: 18 April 2022
Accepted: 25 May 2022
Published: 31 May 2022

1. Introduction

Formation control [1,2] is crucial for multi-agent systems. Previously, switching topology [3,4], actuator faults [5], noise resistance [6], time constraints [7,8], connectivity maintenance [9], and communication delay [10] have been widely studied. Inspired by this research, a stable and feasible controller is critical for the formation control of multi-agent systems. Although various controllers have been proposed, nonlinearity caused by maneuvering [11–13] and saturation [5,14] is still the challenge. Besides, communication interference will lead to bad control due to the lack of reference information, which means extra strategies should be applied for stable formation [4]. Therefore, a comprehensive survey of bounded controllers considering maneuvering and communication interference is necessary. Previously, optimization-based methods and consensus algorithms with graph theory have been widely studied for controller design.

As for controller design, Ref. [14] proposed the inverse optimality method (IOM) with Hamilton–Jacobi–Bellman (HJB) equations, which provides a feasible bounded controller for formation control theoretically, but HJB equations are difficult to be solved for a simple control law. In [15,16], intelligent algorithms have been used to optimize velocities using centralized computing systems. However, time consumption is a big challenge for intelligent algorithms and saturation constraints are hard to be incorporated into the objective functions. Recently, model predictive control (MPC) [17,18] has been widely used for formation control, various requirements can be converted into inequality constraints. MPC is easy to implement programmatically, the challenge is the central computer will assume a great burden with a large number of agents. Then, distributed MPC (DMPC) has been proposed [19,20] for low time cost. With less computation and the advantage of bounded outputs, DMPC has attracted much attention now. The problem with DMPC is that there must exist nonlinear constraints considering dynamic constraints, such as maximum velocity and angular rate, which might cause complex computation. Furthermore, communication interferences will affect MPC and DMPC due to the lack of sufficient information for objective functions and some constraints.

Recently, consensus algorithms (CA) [12,21,22] with graph theory have been extensively researched. With the Laplacian matrix, relationships among agents can be easy to be incorporated into stability analysis with Lyapunov functions (LF), thus the formation switch and stability can be solved simultaneously. CA can apply measurement besides the interacted data to design control laws; what needs to be done is obtaining reference information with limited sources under communication interference [23]. The practicability of CA lies in linear control with linear feedback technique (LFT), with adaptive parameters [5] and sufficient information, the formation can move stably as required. Therefore, insufficient measuring data [1] might cause instability without cooperation, and strategies should be proposed for sufficient reference. To tackle this problem, rigid theory [1,8,11] has been introduced for limited sensors, the formation is expected to be predefined well for obtaining relative bearings or distances solely. However, communication systems and sensors might be equipped for stability in hostile environments, and strategies for obtaining expected information with limited sources can be useful in this situation. More importantly, agents encountering communication break needs to know how many sensing sources are required at least.

Motivated by the above analysis, this paper focuses on the formation control with the following purposes: (1) Establishing a control law with definitely bounded outputs based on LFT technology; thus, the problem of saturation can be avoided by adjusting parameters. (2) Searching for a strategy with insufficient reference, agents encountering communication breaks will obtain sensing data and obtain reference expectedly. In this paper, information processing is introduced for the nonlinear maneuvers [2,11]. Through the coordinate's transformation, virtual reference information including velocity and acceleration are estimated. Then, a nonlinear controller is proposed with the Lyapunov method and the CA algorithm. Given the input saturation, parameters tuning principles of the controller are established based on the Lyapunov method. As for communication breaks, a sensing graph is introduced, and the requirements of the sensing graph are given in terms of various situations. Then, the Laplacian matrix is computed, and the interference resistance ability of agents can be enhanced with the Laplacian matrices of the communication graph. Considering the bearing information only [1], a nonlinear dynamic programming regulator for positions estimation is proposed. Finally, three tests are carried out and the proposed law is proved stable and feasible.

The contributions of this paper are listed below.

(1) A definite bounded control law is proposed for anti-saturation control. The nonlinearity caused by maneuvers is considered compared with [24], then a controller with nonlinear parameters is proposed in this paper. Those parameters are designed as functions of states, and the values space of critical parameters is analyzed subsequently. Differing from the use of auxiliary variables in previous literature, parameters of reference are altered adaptively according to the value of inputs, which will be more applicable and easier to be realized.

(2) A nonlinear dynamic programming regulator is proposed for reference with bearings only for some agents encountering breaks. Instead of expected locations change for all agents, we expect to change the expected locations of agents encountering saturation only for sensing measurements. Thus, most parts of the formation won't be altered if they are not expected to be changed.

The remaining sections are organized as follows. Section 2 describes the problems, and a robust controller is proposed in Section 3. Then, Section 4 uses three tests to verify the proposed strategy. The conclusion is given in Section 5.

Notation: we use $\mathbb{R}^{r\times c}$ to indicate the matrix space of which the matrix has r rows and c columns. $\mathbb{R}^n$ denotes the n-dimensional vector space. $[*]_r^c$ represents the stacked matrix concatenated with elements indicated in the bracket, and $[*]_r^c \in \mathbb{R}^{r\times c}$. $D_1(*)$ indicates the first-time derivative, and $D_2(*)$ indicates the second-time derivative. rank$(*)$ represents the rank of the matrix in the bracket. The matrix operator $\circ$ denotes the Hadamard product and $\otimes$ indicates the Kronecker product operator. $\| * \|_2$ indicates the L2 norm form of the vector, and $\|\boldsymbol{x}\|_{\boldsymbol{M}} = \boldsymbol{x}^{\mathrm{T}}\boldsymbol{M}\boldsymbol{x}$ represents the $\boldsymbol{M}$ norm form of the vector, where $\boldsymbol{M}$ denotes the symmetric positive definite matrix. $\boldsymbol{\Lambda}_L(*)$ indicates the diagonal matrix with size $(L * d_1) \times (L * d_2)$, where (d_1, d_2) is the dimension of the diagonal element in the bracket.

2. Preliminaries

2.1. Graph Theory

For agents i in the agents set $\mathcal{N}_a = \{1, 2, \cdots i, \cdots N\}$ with a predefined formation shape, we define the communication graph as $\mathcal{G} = (\mathcal{V}, \mathcal{E})$, where $\mathcal{V} = \{v_i | i \in \mathcal{N}_a\}$ indicates the vertices, and $\mathrm{E} \subseteq \mathrm{V} \times \mathrm{V}$ represents the edges. Then, adjacent matrix $\boldsymbol{A} = [a_{ij}]_N^N$ is obtained and we have $a_{ij} > 0$ if $(v_i, v_j) \in \mathcal{E}\ \forall i, j \in \mathcal{N}_a$, otherwise $a_{ij} = 0$ and $a_{ii} = 0$. The Laplacian matrix is denoted as $\boldsymbol{\mathcal{L}} = [l_{ij}]_N^N$ with $l_{ii} = -\sum_{i \neq j} a_{ij}$, and $l_{ij} = a_{ij}, \forall i \neq j$.

2.2. Numerical Models and Input Saturation

The dynamic model of agents is given by

$$\begin{cases} \dot{\boldsymbol{X}}_t^i & = f(\boldsymbol{q}_t^i) \\ f(\boldsymbol{q}_t^i) & = [v_t^i cos(\psi_t^i), v_t^i sin(\psi_t^i)] \\ \dot{\boldsymbol{q}}_t^i & = \boldsymbol{u}_t^i \\ \boldsymbol{u}_t^i & = [a_t^i, \omega_t^i]^{\mathrm{T}} \end{cases} \tag{1}$$

where $\boldsymbol{X}_t^i = [x_t^i,\ y_t^i]$ denotes positions, $\boldsymbol{q}_t^i = [v_t^i, \psi_t^i]^{\mathrm{T}}$ represents the velocity expressed with the speed $v_t^i \geq 0$ and the direction $\psi_t^i \in [-2\pi, 2\pi]$, $\boldsymbol{u}_t^i = [a_t^i, \omega_t^i]^{\mathrm{T}}$ indicates the accelerations that will be designed for formation control. The model is nonlinear while considering the maneuvering. Thus, the estimation of $\boldsymbol{u}_t^i$ is vital.

In this paper, CA is applied for controller design, and the distributed feedback law can be indicated as:

$$\boldsymbol{u}_*^i = \sum a_{ij} \Big((\boldsymbol{k}_{ij} \boldsymbol{F}_j(\boldsymbol{\Theta}_j) - \boldsymbol{k}_{ii} \boldsymbol{F}_i(\boldsymbol{\Theta}_i)) + \boldsymbol{w}_{ij} \boldsymbol{p}_{ij} \Big) \tag{2}$$

where $\boldsymbol{u}_*^i$ indicates the desired acceleration, $\boldsymbol{F}_i$ represents the processing functions of interacted information, $\boldsymbol{\Theta}_i = \left(\boldsymbol{X}_t^i, \boldsymbol{q}_t^i, \boldsymbol{u}_t^i\right)$ denotes the interacted information, $\boldsymbol{p}_{ij} \in \mathbb{R}^{n \times 1}$ indicates the expected relative position, $\boldsymbol{k}_{ij} \in \mathbb{R}^{n \times m}$, $\boldsymbol{w}_{ij} \in \mathbb{R}^n$ represent the weight matrix, n indicates the number of the controlled variables, and m represents the dimension of $\boldsymbol{F}_i(\boldsymbol{\Theta}_i)$. Combining $\boldsymbol{\mathcal{L}}$, Equation (2) can be rewritten as:

$$\begin{cases} \boldsymbol{u}_* = (\boldsymbol{K} \circ (\boldsymbol{\mathcal{L}} \otimes \boldsymbol{I}_{n \times m}))\boldsymbol{F} + (\boldsymbol{P} \circ (\boldsymbol{A} \otimes \boldsymbol{1}_{n \times 1}))\boldsymbol{1}_{nN \times 1} \\ \boldsymbol{F} = \left[\boldsymbol{F}_1(\boldsymbol{\Theta}_1)^{\mathrm{T}}, \cdots \boldsymbol{F}_i(\boldsymbol{\Theta}_i)^{\mathrm{T}}, \cdots, \boldsymbol{F}_N(\boldsymbol{\Theta}_N)^{\mathrm{T}}\right]^{\mathrm{T}} \\ P = [\boldsymbol{p}_1{}^{\mathrm{T}}, \boldsymbol{p}_2{}^{\mathrm{T}}, \cdots \boldsymbol{p}_i{}^{\mathrm{T}}, \cdots, \boldsymbol{p}_N{}^{\mathrm{T}}]^{\mathrm{T}} \end{cases} \tag{3}$$

where $\boldsymbol{K} = [\boldsymbol{k}_{ij}]_{Nn}^{Nm}$, $\boldsymbol{p}_i = \left[\boldsymbol{w}_{ij}\boldsymbol{p}_{ij}\right]_n^N$, $\boldsymbol{I}_{n \times m} = [\boldsymbol{I}_n]_n^m$. Where $\boldsymbol{I}_n$ represents the identity matrix, $1_{n \times 1}$ and $1_{nN \times 1}$ are constant matrices with value 1.

Considering the input saturation, the desired output $\boldsymbol{u}_*$ in (3) might not be feasible, and agents cannot realize the desired accelerations provided by the controller. Generally, constraints are placed behind the controller, thus the real inputs $\boldsymbol{u}_f$ of the actuators are restricted. Defining the velocity boundary as $\boldsymbol{q}_{lim}$, then the constraints can be indicated with (4), where k denotes the k-th element.

$$\begin{cases} \boldsymbol{u}_f^i(k) = \boldsymbol{u}_*^i(k), \left|\boldsymbol{u}_*^i(k) + \boldsymbol{q}_t^i(k)\right| \le \boldsymbol{q}_{lim}^i(k) \\ \boldsymbol{u}_f^i(k) = \boldsymbol{u}_*^i(k), \boldsymbol{u}_*^i(k) + \boldsymbol{q}_t^i(k) > \boldsymbol{q}_{lim}^i(k) \\ \boldsymbol{u}_f^i(k) = -\boldsymbol{u}_*^i(k), \boldsymbol{u}_*^i(k) + \boldsymbol{q}_t^i(k) < -\boldsymbol{q}_{lim}^i(k) \end{cases} \tag{4}$$

Constraints in (4) help restrict the outputs, but the parameters of the controller cannot be adjusted timely without adaptive rules, which will hinder the controller from making correct decisions. In this paper, adaptive rules for parameters are proposed in Section 3.2, and $\boldsymbol{u}_*$ will be confined by $\boldsymbol{u}_{lim}$.

2.3. Effect of Communication Break

Given that communication interferences impact interactions among agents, the expected value of coefficients of $\boldsymbol{\mathcal{L}}$ could not be kept unchanged. If all agents can obtain the planned reference information with faults when there exist interferences, methods in [5] can be adopted for motion control. However, there might be communication breaks, and the rank of $\boldsymbol{\mathcal{L}}$ must meet the requirements for formation keeping. Firstly, we give the primary requirements of healthy $\mathcal{G}$.

Lemma 1 [6]. *If $\mathcal{G}$ has a directed spanning forest, then we have rank$(\boldsymbol{\mathcal{L}}) = N - N_l$, where N_l represents the number of distributed networks.*

Proof of Lemma 1 can refer to Remark 2.1 in the literature [6].

Lemma 2. *If there exist communication interferences and rank$(\boldsymbol{\mathcal{L}}) < N - N_l$, where N_l represents the number of distributed networks, then agents cannot keep the expected formation without extra reference information, such as the measurement.*

Proof. According to [6], the Laplacian matrix $\boldsymbol{\mathcal{L}}$ of $\mathcal{G}$ can be split as:

$$\boldsymbol{\mathcal{L}} = \begin{bmatrix} \boldsymbol{0}_{N_l \times N_l} & \boldsymbol{0}_{N_l \times (N - N_l)} \\ \boldsymbol{L}_R & \boldsymbol{L}_F \end{bmatrix} \tag{5}$$

Based on (5), we have rank$(\boldsymbol{\mathcal{L}}) \le N - N_l$. Referring to (3), each row of $\boldsymbol{\mathcal{L}}$ must have non-zero elements if we want all agents can obtain sufficient interacted information for formation control. Next, we assume rank$(\boldsymbol{\mathcal{L}}) < N - N_l$, then there must exist at least one row of $\boldsymbol{\mathcal{L}}_1 = \begin{bmatrix} \boldsymbol{L_R} & \boldsymbol{L_F} \end{bmatrix}$ in which all elements equal 0, which contradicts the demand in Lemma 2. Therefore, Lemma 2 is proved. □

Based on Lemma 2, we have rank$(\boldsymbol{\mathcal{L}}) < N - N_l$ if the communication interference (link failure, block, or strike) causes communication breaks, the system will get out of control. Thus, extra strategies should be provided, which will be discussed in Section 3.3.

3. Main Results

3.1. Reference Information Processing

Firstly, transformations between the inertial coordinate system oxy and the velocity coordinate systems (VOSs) $\left\{o^k x^k y^k \middle| k \in \mathcal{N}_a\right\}$ as shown in Figure 1 are introduced for nonlinear controller design. We use $\{\boldsymbol{\mathcal{T}}_{0i} | i \in \mathcal{N}_a\}$ to indicate the transformation from oxy to VOS, where $\boldsymbol{\mathcal{T}}_{0i} = \boldsymbol{T}(\psi_t^i)$, and $\boldsymbol{T}(\psi_t^i)$ is the rotation matrix.

Assume that the positions can be communicated among agents, we can directly compute $\boldsymbol{q}_t^j$ with $D_1\left(\boldsymbol{X}_t^j\right) = f\left(\boldsymbol{q}_t^j\right)$. Then $\boldsymbol{u}_t^j$ can be estimated by $D_1\left(\boldsymbol{q}_t^j\right)$. However, for the measured information, it is more convenient to estimate $\left(\boldsymbol{q}_t^j, \boldsymbol{u}_t^j\right)$ in VOSs. The relation between $\overset{\sim t}{\boldsymbol{X}}_{ij}$ and $\boldsymbol{q}_t^j$ can be indicated as:

$$D_1\left(\boldsymbol{\mathcal{T}}_{0i}\overset{\sim t}{\boldsymbol{X}}_{ij}\right) = \begin{bmatrix} v_t^j \cos\psi_r^i - v_t^i \\ v_t^j \sin\psi_r^i \end{bmatrix} + D_1(\boldsymbol{\mathcal{T}}_{0i})\overset{\sim t}{\boldsymbol{X}}_{ij} \tag{6}$$

where $\psi_r^i = g\left(\psi_t^i - \psi_t^j\right)$, and $g(\boldsymbol{\varphi}) = \boldsymbol{\varphi}$ if $|\boldsymbol{\varphi}| \leq \pi$, otherwise $g(\boldsymbol{\varphi}) = g(\boldsymbol{\varphi} - sign(\boldsymbol{\varphi}) * 2\pi)$, where $sign(\cdot)$ is the sign function.

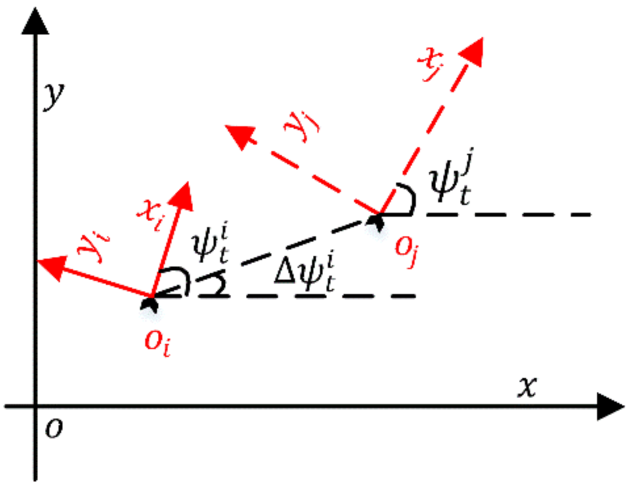

Figure 1. Coordinate transformation.

Referring to (6), v_t^j can be estimated by

$$v_t^j = \| D_1\left(\boldsymbol{\mathcal{T}}_{0i}\overset{\sim t}{\boldsymbol{X}}_{ij}\right) - D_1(\boldsymbol{\mathcal{T}}_{0i})\overset{\sim t}{\boldsymbol{X}}_{ij} + \begin{bmatrix} v_t^i \\ 0 \end{bmatrix} \|_2 \tag{7}$$

Since we obtain v_t^j, ψ_t^j can be computed later. Thus $\overset{\sim j}{\boldsymbol{q}}_t$ is estimated; similarly, we can obtain $\overset{\sim j}{\boldsymbol{u}}_t$. If more information can be interacted, such as $\boldsymbol{q}_t^j$ or $\boldsymbol{u}_t^j$, then unbiased estimations of $\boldsymbol{q}_t^j$ or $\boldsymbol{u}_t^j$ can be realized with the above differential models and extended Kalman filter (EKF).

3.2. Nonlinear Controller Design and Stability Analysis

As can be seen from (6), a high-order controller is required considering the maneuvers during formation acquisition and keeping. In this section, we search for a nonlinear controller without input saturation. Using adaptive parameters, model (3) can be rewritten as $\boldsymbol{u}_* = \boldsymbol{\ell}_f(\boldsymbol{K}, \boldsymbol{\mathcal{L}})\boldsymbol{F} - (\boldsymbol{P} \circ (\boldsymbol{A} \otimes \boldsymbol{1}_{n\times 1}))1_{nN\times 1}$, where $\boldsymbol{F}_i(\boldsymbol{\Theta}_i) = \left[\boldsymbol{X}_t^i, \boldsymbol{q}_t^i, \boldsymbol{u}_t^i\right]^{\mathrm{T}}$, and $\boldsymbol{\ell}_f(\boldsymbol{K}, \boldsymbol{\mathcal{L}})$ indicates the adaptive adjusting function of $\boldsymbol{K}$ and $\boldsymbol{\mathcal{L}}$.

$$\boldsymbol{\ell}_f(\boldsymbol{K}, \boldsymbol{\mathcal{L}}) = -\left[l_{ij}\boldsymbol{k}_{ij}\right] \in \mathbb{R}^{Nn\times Nm} \tag{8}$$

Now, we propose the controller with Proposition 1.

Proposition 1. *For multi-agent systems with strongly connected undirected graph $\mathcal{G}$, the principle of $\boldsymbol{\ell}_f(\boldsymbol{K}, \boldsymbol{\mathcal{L}})$ and $\boldsymbol{P}$ in (8), the controller defined in Equation (3) can guarantee the finite-time stability of the system regardless of communication interference.*

$$\begin{cases} \boldsymbol{k}_{ii} = k_{ij}^1[\boldsymbol{C_K}, \boldsymbol{0}_{2\times4}] \\ \quad + \frac{k_{ij}^2}{l_{ii}v_t^i}\left[\begin{array}{l} \sum v_t^i a_{ij} k_s, -\sum v_t^i a_{ij} k_c, 1, \boldsymbol{0}_{1\times3} \\ \sum a_{ij} k_c, \sum a_{ij} k_s, 0, \boldsymbol{0}_{1\times3} \end{array}\right] \\ \boldsymbol{k}_{ij} = \left[k_{ij}^1 \boldsymbol{C_K}, \boldsymbol{0}_2, \begin{array}{c} cos(\psi_r^i), 0 \\ -\sin(\psi_r^i), k_{ij}^1 \end{array}\right] \\ \quad + \frac{k_{ij}^2}{v_t^i}\left[\begin{array}{l} -v_t^i k_s, v_t^i k_c, v_t^i cos(\psi_r^i), \boldsymbol{0}_{1\times3} \\ -k_c, -k_s, -\sin(\psi_r^i), \boldsymbol{0}_{1\times3} \end{array}\right] \\ \boldsymbol{C_K} = \frac{1}{v_t^i}\left[\begin{array}{l} v_t^i cos(\psi_t^i), v_t^i sin(\psi_t^i) \\ -sin(\psi_t^i), cos(\psi_t^i) \end{array}\right] \\ \boldsymbol{w}_{ij} = k_{ij}^1 \boldsymbol{C_K} + \frac{k_{ij}^2}{v_t^i}\left[\begin{array}{l} -v_t^i k_s, v_t^i k_c \\ -k_c, -k_s \end{array}\right] \end{cases} \tag{9}$$

where $k_s = sin(\psi_t^i)\dot{\psi}_t^j$, $k_c = cos(\psi_t^i)\dot{\psi}_t^j$, *and* k_{ij}^1 *and* k_{ij}^2 *are positive real numbers.*

Before proceeding to the proof of Proposition 1, we introduce Lemma 3.

Lemma 3 [25,26]. *If quadratic scalar function* $V(t)$ *concerning the state of the system satisfies the inequality* $V(t_{k+1}) \le V(t_k) \le V_0 < \infty\ \forall t_0 < t_k < t_{k+1}$ *, the system is progressively stable, where* V_0 *is the value at the initial time* t_0*. The inequality is equivalent to* $\dot{V}(t) \le 0$ *, and the equality holds when* $t_k \ge \tau$ *, where* $\tau > t_0$ *is a positive real number.*

Lemma 4 [27,28]. *If a power scalar function* $V(\boldsymbol{x})$ *is continuously differentiable along* $\boldsymbol{x}$ *with* $\boldsymbol{x} \in \mathbb{R}^n$ *, and the first-order derivative satisfies* $V(\boldsymbol{x}) \le -\gamma_1 V^\alpha(\boldsymbol{x}) - \gamma_1 V(\boldsymbol{x}) - \gamma_1 V^\beta(\boldsymbol{x}) + b_V$ *, where* $\sum\limits_{k=1,2,3} \gamma_k \ne 0$ *,* $0 < \alpha < 1 < \beta$ *,* b_V *is a bounded positive number. Then* $\boldsymbol{x}$ *will approach the equilibrium state in a finite time.*

Next, we give the proof of Proposition 1.

Proof. Firstly, we introduce the combined vector $\overset{\sim t}{\boldsymbol{X}}_i$, $\overset{\sim t}{\boldsymbol{Z}}_i$, and permutation matrix $\boldsymbol{P}_e^t$, where $\overset{\sim t}{\boldsymbol{X}}_i = \left(\left[\overset{\sim t}{\boldsymbol{X}}_{ij}{}^{\mathrm{T}}\right]_1^{nN}\right)^{\mathrm{T}}$, $\overset{\sim t}{\boldsymbol{Z}}_i = \left[\overset{\sim t}{\boldsymbol{X}}_{ij}\right]_n^N$, and $\boldsymbol{P}_e^t$ satisfies:

$$\overset{\sim t}{\boldsymbol{Z}}_i \boldsymbol{P}_e^t = \left[\overset{\sim \mathcal{L}_t}{\boldsymbol{Z}_i} \quad \overset{\sim \mathcal{O}_t}{\boldsymbol{Z}_i}\right] \tag{10}$$

where $\overset{\sim \mathcal{L}_t}{\boldsymbol{Z}_i} = \left[\overset{\sim t}{\boldsymbol{X}}_{ij_k}\right]_n^L$, $\overset{\sim \mathcal{O}_t}{\boldsymbol{Z}_i} = \left[\overset{\sim t}{\boldsymbol{X}}_{ij_k}\right]_n^{N-L}$, $k = 1, 2, \cdots, N$. $\overset{\sim \mathcal{L}_t}{\boldsymbol{Z}_i}$ represents the interacted information from nearby agents, and $\overset{\sim \mathcal{O}_t}{\boldsymbol{Z}_i}$ denotes the information of agents without interaction which is impossible to obtain. Reshaping $\overset{\sim t}{\boldsymbol{Z}}_i \boldsymbol{P}_e^t$ yields:

$$\phi\left(\overset{\sim t}{\boldsymbol{Z}}_i \boldsymbol{P}_e^t\right) = \left[\overset{\sim \mathcal{L}_t}{\boldsymbol{X}_i} \quad \overset{\sim \mathcal{O}_t}{\boldsymbol{X}_i}\right]^{\mathrm{T}} \tag{11}$$

where $\overset{\sim \mathcal{L}_t}{\boldsymbol{X}_i} = \left[\overset{\sim t}{\boldsymbol{X}}_{ij_k}{}^{\mathrm{T}}\right]_1^{nL}$, $\overset{\sim \mathcal{O}_t}{\boldsymbol{X}_i} = \left[\overset{\sim t}{\boldsymbol{X}}_{ij_k}\right]_n^N$.

Define the rotation matrices $\boldsymbol{Q}_i^t$ with $\boldsymbol{\mathcal{T}}_{0i}^{\mathcal{L}} = \boldsymbol{\Lambda}_L(\boldsymbol{\mathcal{T}}_{\mathbf{0}j_1})$.

$$\boldsymbol{Q}_i^t = \begin{bmatrix} \boldsymbol{\mathcal{T}}_{0i}^{\mathcal{L}} & \mathbf{0} \\ \mathbf{0} & \mathbf{0} \end{bmatrix} \tag{12}$$

Define the Lyapunov function $V^i(t) = V_1^i(t) + V_2^i(t)$ with

$$\begin{cases} V_1^i(t) = \frac{1}{2}\left(\boldsymbol{Q}_i^t \boldsymbol{\phi}\left(\overset{\sim t}{\boldsymbol{Z}}_i \boldsymbol{P}_e^t\right)\right)^{\mathrm{T}} \boldsymbol{R}_1 \boldsymbol{Q}_i^t \boldsymbol{\phi}\left(\overset{\sim t}{\boldsymbol{Z}}_i \boldsymbol{P}_e^t\right) \\ V_2^i(t) = \frac{1}{2}\left(\overset{\sim t}{\boldsymbol{q}}_i\right)^{\mathrm{T}} \boldsymbol{R}_2 \overset{\sim t}{\boldsymbol{q}}_i \end{cases} \tag{13}$$

where $\overset{\sim t}{\boldsymbol{q}}_i = D_1\left(\boldsymbol{Q}_i^t \boldsymbol{\phi}\left(\overset{\sim t}{\boldsymbol{Z}}_i \boldsymbol{P}_e^t\right)\right)$, and matrices $(\boldsymbol{R}_1,\ \boldsymbol{R}_2)$ satisfy:

$$\begin{cases} \boldsymbol{R}_1 = \mathrm{diag}\left(\boldsymbol{\Lambda}_L\left(\eta_{j_k} a_{ij_k}\right), \mathbf{0}_{N-L}\right) \otimes \boldsymbol{I}_2 \\ \boldsymbol{R}_2 = \eta_0 \mathrm{diag}\left(\boldsymbol{\Lambda}_L\left(\eta_{j_k} a_{ij_k}\right), \mathbf{0}_{N-L}\right) \otimes \boldsymbol{I}_2 \end{cases} \tag{14}$$

With $\mathrm{diag}(\cdot)$ being a diagonal matrix, $\mathbf{0}_{N-L}$ being a zero matrix, and $\{\eta_i\}_0^{L+1}$ being positive real numbers.

Taking the derivative of (12), we have:

$$\begin{cases} \dot{V}_1^i(t) = \left(\boldsymbol{Q}_i^t \phi\left(\overset{\sim t}{\boldsymbol{Z}}_i P_e^t\right)\right)^{\mathrm{T}} \boldsymbol{R}_1 \overset{\sim t}{\boldsymbol{q}}_i \\ \qquad = \left(\boldsymbol{\mathcal{T}}_{0i}^{\mathcal{L}} \overset{\sim \mathcal{L}_t}{\boldsymbol{X}_i}\right)^{\mathrm{T}} \left(\boldsymbol{\Lambda}_L\left(\eta_{j_k} a_{ij_k}\right) \otimes \boldsymbol{I}_2\right) \overset{\sim \mathcal{L}_t}{\boldsymbol{q}_i} \\ \dot{V}_2^i(t) = \eta_0 \left(\overset{\sim \mathcal{L}_t}{\boldsymbol{q}_i}\right)^{\mathrm{T}} \left(\boldsymbol{\Lambda}_L\left(\eta_{j_k} a_{ij_k}\right) \otimes \boldsymbol{I}_2\right) D_1\left(\overset{\sim \mathcal{L}_t}{\boldsymbol{q}_i}\right) \end{cases} \tag{15}$$

with $\overset{\sim \mathcal{L}_t}{\boldsymbol{q}_i} = D_1\left(\boldsymbol{\mathcal{T}}_{0i}^{\mathcal{L}} \overset{\sim \mathcal{L}_t}{\boldsymbol{X}_i}\right)$.

Then, we obtain

$$\begin{aligned} \dot{V}^i(t) = & \left(\boldsymbol{\mathcal{T}}_{0i}^{\mathcal{L}} \overset{\sim \mathcal{L}_t}{\boldsymbol{X}_i}\right)^{\mathrm{T}} \left(\boldsymbol{\Lambda}_L\left(\eta_{j_k} a_{ij_k}\right) \otimes \boldsymbol{I}_2\right) \overset{\sim \mathcal{L}_t}{\boldsymbol{q}_i} \\ & + \eta_0 \left(\overset{\sim \mathcal{L}_t}{\boldsymbol{q}_i}\right)^{\mathrm{T}} \left(\boldsymbol{\Lambda}_L\left(\eta_{j_k} a_{ij_k}\right) \otimes \boldsymbol{I}_2\right) D_1\left(\overset{\sim \mathcal{L}_t}{\boldsymbol{q}_i}\right) \end{aligned} \tag{16}$$

Before proceeding to the next step, we rewrite $\boldsymbol{u}_*^i$ as

$$\begin{aligned} \boldsymbol{u}_*^i = & \boldsymbol{E}_i \boldsymbol{\ell}_f(\boldsymbol{K}, \boldsymbol{\mathcal{L}}) \boldsymbol{F} \\ & - \boldsymbol{E}_i(\boldsymbol{P} \circ (\boldsymbol{A} \otimes \mathbf{1}_{n \times 1})) \mathbf{1}_{nN \times 1} = \sum \boldsymbol{u}_{ij_k}^t \end{aligned} \tag{17}$$

where $\boldsymbol{E}_i = [\boldsymbol{e}_1, \cdots, \boldsymbol{e}_N] \in \mathbb{R}^{n \times nN}$, $\boldsymbol{e}_i = \boldsymbol{I}_2$, $\boldsymbol{e}_{j \neq i} = \mathbf{0}_2$.

$\overset{\sim \mathcal{L}_t}{\boldsymbol{q}_i}$ can be rearranged as

$$\begin{aligned} \overset{\sim \mathcal{L}_t}{\boldsymbol{q}_i} & = D_1\left(\boldsymbol{\mathcal{T}}_{0i}^{\mathcal{L}} \overset{\sim \mathcal{L}_t}{\boldsymbol{X}_i}\right) \\ & = \overset{\sim \mathcal{L}}{\boldsymbol{\mathcal{T}}}_{0i} \otimes \boldsymbol{P}_{e1} \overset{\sim \mathcal{L}_t}{\boldsymbol{X}_i} + \boldsymbol{\beta}_i^1 \boldsymbol{q}_i^{\mathcal{L}_t} + \mathbf{1}_{L \times 1} \otimes \boldsymbol{P}_1 \boldsymbol{q}_t^i \end{aligned} \tag{18}$$

With $\boldsymbol{q}_i^{\mathcal{L}_t} = \left(\left[\left(\boldsymbol{q}_t^{j_k}\right)^{\mathrm{T}}\right]_1^{nN}\right)^{\mathrm{T}}$, $\boldsymbol{P}_{e1} = \begin{bmatrix} 0 & 1 \\ -1 & 0 \end{bmatrix}$, $\boldsymbol{P}_1 = \begin{bmatrix} -1 & 0 \\ 0 & 0 \end{bmatrix}$, $\boldsymbol{\beta}_{j_k}^1 = \begin{bmatrix} cos\left(\psi_r^{ij_k}\right) & 0 \\ sin\left(\psi_r^{ij_k}\right) & 0 \end{bmatrix}$, $\overset{\sim \mathcal{L}}{\boldsymbol{\mathcal{T}}}_{0i} = \boldsymbol{\Lambda}_L\left(\boldsymbol{\mathcal{T}}_{0j_k} \dot{\psi}_t^{j_k}\right)$, $\boldsymbol{\beta}_i^1 = \boldsymbol{\Lambda}_L\left(\beta_{j_k}^1\right)$.

Referring to (17) and (18), we have

$$D_1\left(\tilde{\boldsymbol{q}}_i^{\mathcal{L}_t}\right) = (\boldsymbol{I}_L \otimes \boldsymbol{P}_e)\left(\tilde{T}_{ij}^{\mathcal{L}} \otimes \boldsymbol{P}_2\right)\boldsymbol{u}_i^{\mathcal{L}_t} + \tilde{\boldsymbol{\varphi}}_i^{\mathcal{L}}\tilde{\boldsymbol{q}}_i^{\mathcal{L}_t} - \beta_i^2 D_1\left(\boldsymbol{q}_i^{\mathcal{L}_t}\right) \tag{19}$$

With $\boldsymbol{u}_i^{\mathcal{L}_t} = \left(\left[\boldsymbol{u}_{ij_k}^{t}{}^{\mathrm{T}}\right]_1^{nN}\right)^{\mathrm{T}}$, $\boldsymbol{P}_e = \begin{bmatrix} 0 & 1 \\ 1 & 0 \end{bmatrix}$, $\boldsymbol{P}_2 = \begin{bmatrix} 0 & v_t^i \\ 1 & 0 \end{bmatrix}$, $\beta_{j_k}^2 = \begin{bmatrix} 1 & 0 \\ sin\left(\psi_r^{ij_k}\right) & v_t^i cos\left(\psi_r^{ij_k}\right) \end{bmatrix}$, $\tilde{T}_{ij}^{\mathcal{L}} = \boldsymbol{\Lambda}_L\left(T\left(\psi_r^{ij_1}\right)\right)$, $\beta_i^2 = \boldsymbol{\Lambda}_L\left(\beta_{j_k}^2\right)$, $\tilde{\boldsymbol{\varphi}}_i^{\mathcal{L}} = \boldsymbol{\Lambda}_L\left(\dot{\psi}_t^{j_1}\right) \otimes \boldsymbol{P}_{e1}$.

Subsequently, $\dot{V}^i(t)$ can be rewritten as:

$$\begin{cases} \dot{V}^i(t) = \left(\boldsymbol{\mathcal{T}}_{0i}^{\mathcal{L}}\tilde{\boldsymbol{X}}_i^{\mathcal{L}_t}\right)^{\mathrm{T}}\left(\boldsymbol{\Lambda}_L\left(\eta_{j_k}a_{ij_k}\right) \otimes \boldsymbol{I}_2\right)\tilde{\boldsymbol{q}}_i^{\mathcal{L}_t} \\ \qquad +\gamma_k(\boldsymbol{I}_L \otimes \boldsymbol{P}_e)\left(\tilde{\boldsymbol{T}}_{ij}^{\mathcal{L}} \otimes \boldsymbol{P}_2\right)\boldsymbol{u}_*^{i\mathcal{L}_t} \\ \qquad -\gamma_k(\boldsymbol{I}_L \otimes \boldsymbol{P}_e)\left(\tilde{\boldsymbol{T}}_{ij}^{\mathcal{L}} \otimes (\boldsymbol{P}_e\boldsymbol{P}_1\boldsymbol{P}_e)\right)D_1\left(\boldsymbol{q}_i^{\mathcal{L}_t}\right) \\ \qquad +\gamma_k\left(\tilde{\boldsymbol{\varphi}}_i^{\mathcal{L}}\tilde{\boldsymbol{q}}_i^{\mathcal{L}_t} + \boldsymbol{I}_L \otimes \boldsymbol{P}_1 D_1\left(\boldsymbol{q}_i^{\mathcal{L}_t}\right)\right) \\ \gamma_k = \eta_0\left(\tilde{\boldsymbol{q}}_i^{\mathcal{L}_t}\right)^{\mathrm{T}}\left(\boldsymbol{\Lambda}_L\left(\eta_{j_k}a_{ij_k}\right) \otimes \boldsymbol{I}_2\right) \end{cases} \tag{20}$$

where $\boldsymbol{u}_i^{\mathcal{L}_t}$ can be rewritten as

$$\begin{aligned} \boldsymbol{u}_i^{\mathcal{L}_t} &= \tilde{\boldsymbol{K}}_i^2 \boldsymbol{1}_{L\times 1} \otimes \boldsymbol{P}_1 k_i^2 \boldsymbol{q}_t^i + \tilde{\boldsymbol{K}}_i^3 \boldsymbol{q}_i^{\mathcal{L}_t} + \tilde{\boldsymbol{K}}_i^4 D_1\left(\boldsymbol{q}_i^{\mathcal{L}_t}\right) \\ &\quad -\left(\tilde{\boldsymbol{K}}_i^1 \otimes \boldsymbol{\lambda}_i^1\boldsymbol{\mathcal{T}}_{0i} + \acute{\boldsymbol{T}}_{0i}^{\mathcal{L}} \otimes \left((\boldsymbol{P}_{e1})^{\mathrm{T}}\boldsymbol{\mathcal{T}}_{0i}\right)\right)\tilde{\boldsymbol{X}}_i^{\mathcal{L}_t} \end{aligned} \tag{21}$$

With $\acute{\boldsymbol{T}}_{0i}^{\mathcal{L}} = l_{ii}\boldsymbol{\Lambda}_L\left(k_{ij_k}^2\lambda_{ij_k}\right)$, $\tilde{\boldsymbol{K}}_i^1 = \boldsymbol{\Lambda}_L\left(k_{ij_k}^1\right)$, $\tilde{\boldsymbol{K}}_i^2 = \left[k_{ij_k}^1\right]_L^1$, $\tilde{\boldsymbol{K}}_i^3 = \boldsymbol{\Lambda}_L\left(k_{ij_k}^2 k_{ij_k}^2\right)$, $\tilde{\boldsymbol{K}}_i^4 = \boldsymbol{\Lambda}_L\left(k_{ij_k}^3\right)$.

Redefining $\boldsymbol{k}_{ii}$ and $\boldsymbol{k}_{ij_k}$ as $\boldsymbol{k}_{ii} = \left[\boldsymbol{k}_{ii}^1, \boldsymbol{k}_{ii}^2, 0_3\right]$ and $\boldsymbol{k}_{ij_k} = \left[\boldsymbol{k}_{ij_k}^1, \boldsymbol{k}_{ij_k}^2, \boldsymbol{k}_{ij_k}^3\right]$ with

$$\begin{cases} \boldsymbol{k}_{ii}^1 = \sum_{j\neq i} k_{ij}^1\boldsymbol{\lambda}_i^1\boldsymbol{\mathcal{T}}_{0i} - \sum_{j\neq i} k_{ij}^2\lambda_{ij}\boldsymbol{P}_e\boldsymbol{\mathcal{T}}_{0i} \\ \boldsymbol{k}_{ij_k}^1 = k_{ij}^1\boldsymbol{\lambda}_i^1\boldsymbol{\mathcal{T}}_{0i} - k_{ij}^2\lambda_{ij}\boldsymbol{P}_e\boldsymbol{\mathcal{T}}_{0i} \\ \boldsymbol{k}_{ii}^2 = \begin{bmatrix} k_{ij}^2 \\ 0 \end{bmatrix}, \boldsymbol{k}_{ij_k}^2 = \frac{1}{v_t^i}\begin{bmatrix} cos\left(\psi_r^{ij_k}\right)v_t^i & 0 \\ -\sin\left(\psi_r^{ij_k}\right) & 0 \end{bmatrix} \\ \boldsymbol{k}_{ij_k}^3 = \frac{1}{v_t^i}\begin{bmatrix} cos\left(\psi_r^{ij_k}\right)v_t^i & 0 \\ -\sin\left(\psi_r^{ij_k}\right) & v_t^i \end{bmatrix} \end{cases} \tag{22}$$

where $\boldsymbol{\lambda}_i^1 = \frac{1}{l_{ii}v_t^i}\begin{bmatrix} v_t^i & 0 \\ 0 & 1 \end{bmatrix}$, $\boldsymbol{\lambda}_{ij} = \frac{-1}{l_{ii}v_t^i}\begin{bmatrix} \dot{\psi}_t^j v_t^i & 0 \\ 0 & \dot{\psi}_t^j \end{bmatrix}$.

Next, we have

$$\begin{aligned}
\dot{V}^{i}(t) = {} & \eta_0 \textstyle\sum_{k=1}^{L} \gamma_{ij_k} \boldsymbol{P_T} \boldsymbol{k}_{ij_k}^{2} \boldsymbol{q}_t^{j_k} \\
& + \eta_0 \left(\widetilde{\boldsymbol{q}}_i^{\mathcal{L}_t} \right)^{\mathrm{T}} \boldsymbol{\Lambda}_L \left(\eta_{j_k} a_{ij_k} \right) \widetilde{\boldsymbol{\varphi}}_i^{\mathcal{L}} \widetilde{\boldsymbol{q}}_i^{\mathcal{L}_t} \\
& - \eta_0 \textstyle\sum_{k=1}^{L} \gamma_{ij_k} \boldsymbol{P_T} l_{ii} \boldsymbol{\lambda}_{ij_k} \left(\boldsymbol{P}_{e1} \right)^{\mathrm{T}} \boldsymbol{\mathcal{T}}_{0i} \widetilde{\boldsymbol{X}}_{ij_k}^{t} \\
& \eta_0 \textstyle\sum_{k=1}^{L} \left(\gamma_{ij_k} \boldsymbol{\zeta}_{ij_k} D_1 \left(\boldsymbol{q}_t^{j_k} \right) + \gamma_{ij_k} \boldsymbol{P_T} \boldsymbol{P}_1 \boldsymbol{q}_t^{i} \right) \\
& + \textstyle\sum_{k=1}^{L} \left(\eta_{j_k} - \eta_0 k_{ij_k}^{1} \right) \left(\boldsymbol{\mathcal{T}}_{0j_k} \widetilde{\boldsymbol{X}}_{ij_k}^{t} \right)^{\mathrm{T}} \left(\gamma_{ij_k} \right)^{\mathrm{T}}
\end{aligned} \tag{23}$$

where

$$\begin{cases}
\gamma_{ij_{\boldsymbol{k}}} = \left(\widetilde{\boldsymbol{q}}_{ij_k}^{t} \right)^{\mathrm{T}} \left(a_{ij_k} \boldsymbol{I}_2 \right), \boldsymbol{P_T} = \boldsymbol{P}_e \boldsymbol{T} \left(\psi_r^{ij_k} \right) \boldsymbol{P}_2 \\
\zeta_{ij_k} = \boldsymbol{P_T} \boldsymbol{k}_{ij_k}^{3} - \boldsymbol{P}_e \boldsymbol{T} \left(\psi_r^{ij_k} \right) \boldsymbol{P}_e \boldsymbol{P}_1 \boldsymbol{P}_e + \boldsymbol{P}_1
\end{cases}$$

Furthermore, $\dot{V}^{i}(t)$ can be simplified as

$$\begin{aligned}
\dot{V}^{i}(t) = {} & \eta_0 \textstyle\sum_{k=1}^{L} \gamma_{ij_k} \overline{\zeta}_{ij_k} D_1 \left(\boldsymbol{q}_t^{j_k} \right) \\
& + \eta_0 \left(\widetilde{\boldsymbol{q}}_i^{\mathcal{L}_t} \right)^{\mathrm{T}} \left(\boldsymbol{\Lambda}_L \left(\eta_{j_k} a_{ij_k} \right) \otimes \boldsymbol{I}_2 \right) \widetilde{\boldsymbol{\varphi}}_i^{\mathcal{L}} \widetilde{\boldsymbol{q}}_i^{\mathcal{L}_t} \\
& + \textstyle\sum_{k=1}^{L} \left(\eta_{j_k} - \eta_0 k_{ij_k}^{1} \right) \left(\boldsymbol{\mathcal{T}}_{0j_k} \widetilde{\boldsymbol{X}}_{ij_k}^{t} \right)^{\mathrm{T}} \left(\gamma_{ij_k} \right)^{\mathrm{T}} \\
= {} & \textstyle\sum_{k=1}^{L} \left(\eta_{j_k} - \eta_0 k_{ij_k}^{1} \right) \left(\boldsymbol{\mathcal{T}}_{0j_k} \widetilde{\boldsymbol{X}}_{ij_k}^{t} \right)^{\mathrm{T}} \left(\gamma_{ij_k} \right)^{\mathrm{T}} \\
& + \eta_0 \left(\widetilde{\boldsymbol{q}}_i^{\mathcal{L}_t} \right)^{\mathrm{T}} \left(\boldsymbol{\Lambda}_L \left(\eta_{j_k} a_{ij_k} \right) \otimes \boldsymbol{I}_2 \right) \widetilde{\boldsymbol{\varphi}}_i^{\mathcal{L}} \widetilde{\boldsymbol{q}}_i^{\mathcal{L}_t} \\
& - \eta_0 \left(\widetilde{\boldsymbol{q}}_i^{\mathcal{L}_t} \right)^{\mathrm{T}} \left(\boldsymbol{\Lambda}_L \left(\eta_{j_k} a_{ij_k} \right) \otimes \boldsymbol{I}_2 \right) \widetilde{\boldsymbol{q}}_i^{\mathcal{L}_t}
\end{aligned} \tag{24}$$

where

$$\overline{\zeta}_{ij_k} = \boldsymbol{\mathcal{T}}_{0j} \boldsymbol{P}_{e1} \widetilde{\boldsymbol{X}}_{ij_k}^{t} - \left(\boldsymbol{T} \left(\psi_r^{ij_k} \right) \right)^{\mathrm{T}} \boldsymbol{P}_1 \boldsymbol{q}_t^{i} + \boldsymbol{P}_1 \boldsymbol{q}_t^{j_k}$$

Utilizing the equality $\left(\widetilde{\boldsymbol{q}}_i^{\mathcal{L}_t} \right)^{\mathrm{T}} \left(\boldsymbol{\Lambda}_L \left(\eta_{j_k} a_{ij_k} \right) \otimes \boldsymbol{I}_2 \right) \widetilde{\boldsymbol{\varphi}}_i^{\mathcal{L}} \widetilde{\boldsymbol{q}}_i^{\mathcal{L}_t} = 0$ and choosing $\eta_{j_k} = \eta_0 k_{ij_k}^{1}$, we have $\dot{V}^{i}(t) \leq 0$ and the equality holds only if $\widetilde{\boldsymbol{q}}_i^{\mathcal{L}_t}$ equals zero. According to Lemma 3, the system must be asymptotical stable, and the tracking errors are decreasing. Thus, $\boldsymbol{\phi} \left(\widetilde{\boldsymbol{Z}}_i^{t} \boldsymbol{P}_e^{t} \right)$ is bounded and there exists a positive number B_V that satisfies $V_1^i(t) \leq b_V$. Therefore, we have $\dot{V}^{i}(t) \leq -k_V V^i(t) + k_V B_V$, where k_V is a positive real number. Consequently, $V^i(t)$ will converge to an equilibrium state in a finite time based on Lemma 4.

The proof of Proposition 1 is finished. □

3.3. Adaptive Rules for Parameters

Referring to (4), we have $v_-(t) \leq v_i(t) \leq v_+(t)\ \forall i \in \mathcal{N}_a$, where $v_-(t)$ indicates the lower limit of $v_i(t)$, and $v_+(t) > 0$ is the upper limit. In addition, $v_-(t)$ and $v_+(t)$ are time varying but satisfy the constraint $-v_m \leq v_-(t) \leq v_+(t) \leq v_m$.

Theorem 1. *If $V(t)$ is the quadratic scalar function with the derivative $\dot{V}(t) = -\pi_1 V(t) \pm \sqrt{V(t)}\pi(t)$, where $\pi_1 > 0$ and $\pi(t)$ satisfies the inequation $-\pi_m \leq \pi_-(t) \leq \pi(t) \leq \pi_+(t) \leq \pi_m$, then $V(t)$ is bounded by $\sqrt{V(t)} \leq \pi_m$.*

Proof. Handling the derivative, we have $\dot{V}(t) = \sqrt{V(t)}\left(-\pi_1\sqrt{V(t)} \pm \pi(t)\right)$. Using the condition $-\pi_m \le \pi_-(t) \le \pi(t) \le \pi_+(t) \le \pi_m$ yields $\dot{V}(t) \le \sqrt{V(t)}\left(-\pi_1\sqrt{V(t)} + \pi_m\right)$, we obtain the result $\sqrt{V(t)} \le \pi_m$ referring to Lemma 4. □

Proposition 2. *Define the max acceleration, angular rate, and velocity as a_m, ω_m, and v_m, respectively, with $\left|a_t^i\right| \le a_i \le a_m, \left|\omega_t^i\right| \le \omega_i \le \omega_m, \left|v_t^i\right| \le v_i \le v_m$. Then, the velocity of agents must be bounded if $k_{ij_k}^1 = \frac{\alpha_{j_k}}{d_{j_k}(t)}$ and $k_{ij_k}^2 = \beta_{j_k} k_{ij_k}^1$ hold with α_{j_k},β_{j_k}, and d_{j_k} satisfying the following equations.*

$$\begin{aligned} &\alpha_{j_k} + \alpha_{j_k}\beta_{j_k}\left|\omega_{j_k}\right| \\ &\le \sqrt{0.5\left(\left(2k_{ij_k}^2 v_m\right)^2 - 0.5\left(k_{ij_k}^2 v_{j_k} + a_{j_k}\right)^2\right)} \end{aligned} \tag{25}$$

$$2k_{ij_k}^2 v_m \ge \left|k_{ij_k}^2 v_{j_k} + a_{j_k}\right| \tag{26}$$

Remark 1. *d_{j_k} is correlated to $\overset{\sim t}{\boldsymbol{X}}_{ij}$, because $V(t)$ is asymptotically convergent, which means $V_{j_k}(t) = \eta_{j_k}\left(\boldsymbol{\mathcal{T}}_{0j_k}\overset{\sim t}{\boldsymbol{X}}_{ij_k}\right)^T \boldsymbol{\mathcal{T}}_{0j_k}\overset{\sim t}{\boldsymbol{X}}_{ij_k} + \eta_0\eta_{j_k}\left(\overset{\sim t}{\boldsymbol{q}}_{ij_k}\right)^T \overset{\sim t}{\boldsymbol{q}}_{ij_k}$ is decreasing. Here, we can choose the positive variable $d_{j_k}(t) = d_{j_k}(t_0)$, where $\sqrt{V_{j_k}(t_0)} \le d_{j_k}(t_0)$, so we can obtain $\sqrt{V_{j_k}(t)} \le d_{j_k}(t_0)$, thus $\left|\overset{\sim t}{\boldsymbol{X}}_{ij}\right| \le d_{j_k}(t_0)\mathbf{1}_{1\times 2}$.*

Remark 2. *Since $\left|v_{j_k}\right| \le v_m$,$k_{ij_k}^2\left(2v_m - \left|v_{j_k}\right|\right) \ge \left|a_{j_k}\right|$ can be realized, which means we can obtain positive α_{j_k} and β_{j_k} for bounded controller design.*

Proof of Proposition 2. Based on the law (3), we can obtain:

$$\begin{aligned} \dot{v}_t^i = &-\sum_{k=1}^{L}\begin{bmatrix} k_{ij_k}^1 & k_{ij_k}^2 & \dot{\psi}_t^{j_k} \end{bmatrix}\boldsymbol{\mathcal{T}}_{0i}\overset{\sim t}{\boldsymbol{X}}_{ij_k} \\ &-\sum_{k=1}^{L} k_{ij_k}^2\left(v_t^i - v_t^{j_k}cos\left(\psi_r^{ij_k}\right)\right) - cos\left(\psi_r^{ij_k}\right)a_t^{j_k} \end{aligned} \tag{27}$$

Introducing Lyapunov function V_3:

$$V_3(t) = \tfrac{1}{2}\left(v_t^i\right)^2 \tag{28}$$

Based on Equation (30), the derivative of V_3 can be obtained:

$$\begin{aligned} \dot{V}_3(t) = &-2k_p^v\left(v_t^i\right)^2 + v_t^i\sum_{k=1}^{L} cos\left(\psi_r^{ij_k}\right)a_t^{j_k} \\ &+v_t^i\sum_{k=1}^{L} k_{ij_k}^2 v_t^{j_k} cos\left(\psi_r^{ij_k}\right) \\ &+v_t^i\sum_{k=1}^{L} -\begin{bmatrix} k_{ij_k}^1 & k_{ij_k}^2\dot{\psi}_t^{j_k} \end{bmatrix}\boldsymbol{\mathcal{T}}_{0i}\overset{\sim t}{\boldsymbol{X}}_{ij_k} \\ &= -2k_p^v\left(v_t^i\right)^2 + v_t^i\sum_{k=1}^{L}\pi_t^{ij_k} \end{aligned} \tag{29}$$

where $k_p^v = \sum_{k=1}^{L} k_{ij_k}^2$, $\pi_t^i = -\begin{bmatrix} k_{ij_k}^1 & k_{ij_k}^2\dot{\psi}_t^{j_k} \end{bmatrix}\boldsymbol{\mathcal{T}}_{0i}\overset{\sim t}{\boldsymbol{X}}_{ij_k} + cos\left(\psi_r^{ij_k}\right)a_t^{j_k} + k_{ij_k}^2 v_t^{j_k} cos\left(\psi_r^{ij_k}\right)$. Using $\boldsymbol{\mathcal{T}}_{0i}\overset{\sim t}{\boldsymbol{X}}_{ij_k} = \boldsymbol{T}\left(\psi_r^{ij_k}\right)\boldsymbol{\mathcal{T}}_{0i}\overset{\sim t}{\boldsymbol{X}}_{ij_k}$ and defining $\boldsymbol{\mathcal{T}}_{0i}\overset{\sim t}{\boldsymbol{X}}_{ij_k} = \left[x_{ij_k}^e(t), y_{ij_k}^e(t)\right]^{\mathrm{T}}$, we have

$$\pi_t^{ij_k} = -sin\left(\psi_r^{ij_k}\right)a_{j_k}(t) - cos\left(\psi_r^{ij_k}\right)b_{j_k}(t) \tag{30}$$

where

$$\begin{cases} a_{j_k}(t) = k^1_{ij_k} y^e_{ij_k}(t) - k^2_{ij_k} x^e_{ij_k}(t)\dot{\psi}^{j_k}_t \\ b_j(t) = -a^{j_k}_t - k^2_{ij_k} v^{j_k}_t \\ \qquad k^1_{ij_k} x^e_{ij_k}(t) + k^2_{ij_k} y^e_{ij_k}(t)\dot{\psi}^{j_k}_t \end{cases}$$

Firstly, we give the following in Equation (31):

$$\begin{aligned} &\left|-sin\left(\psi^{ij_k}_r\right)a_{j_k}(t) - cos\left(\psi^{ij_k}_r\right)b_{j_k}(t)\right| \\ &\leq \sqrt{\left(a_{j_k}(t)\right)^2 + \left(b_{j_k}(t)\right)^2} \end{aligned} \tag{31}$$

Assuming $x = \left|sin\left(\psi^{ij_k}_r\right)\right|$ yields the function $f_x = \left|a_{j_k}(t)\right|x + b_{j_k}(t)\sqrt{1-x^2}, 0 \leq x \leq 1$. Then, taking the derivative of f_x, we have:

$$\dot{f}_x = \left|a_{j_k}(t)\right| - \frac{b_{j_k}(t)x}{\sqrt{1-x^2}} \tag{32}$$

Referring to (32), f_x is maximum when $x\sqrt{\left(a_{j_k}(t)\right)^2 + \left(b_{j_k}(t)\right)^2} = \left|a_{j_k}(t)\right|$. Defining $\sigma_{j_k} = \alpha_{j_k} + \alpha_{j_k}\beta_{j_k}\left|\omega_{j_k}\right|$, we have the following inequation based on (30) and Theorem 1:

$$\begin{aligned} &\left|\pi^{ij_k}_t\right| \leq \sqrt{\left(a_{j_k}(t)\right)^2 + \left(b_{j_k}(t)\right)^2} \\ &\leq \sqrt{2\left(\sigma_{j_k}\right)^2 + \left|k^2_{ij_k} v_{j_k} + a_{j_k}\right|^2 + 2\left|k^2_{ij_k} v_{j_k} + a_{j_k}\right|\sigma_{j_k}} \end{aligned} \tag{33}$$

Consequently, $\left|\pi^{ij_k}_t\right| \leq 2k^v_p v_m$ holds and we can obtain $v^i_t \leq v_m$ with $\pi^{ij_k}_t > 0$ or $v^i_t \geq -v_m$ with $\pi^{ij_k}_t > 0$. Based on the equality $a_{ij_k}(t_{k+1}) = \pi^{ij_k}_{t_k} - k^2_{ij_k} v^i_{t_k}$ and the inequality $v^i_{t_k} \geq v_- \geq 0$, we have $v^i_{t_{k+1}} \geq -v_m$ with $\left|v^i_{t_k}\right| \leq v_m$ and $\pi^{ij_k}_{t_k} \leq 0$, or $v^i_{t_{k+1}} \leq v_m$ with $\left|v^i_{t_k}\right| \leq v_m$ and $\pi^{ij_k}_{t_k} \geq 0$. Thus, the velocity constraint can be satisfied with the condition $v^i_{t_k} \geq v_- \geq 0$, the challenge is how to make sure that $\left(\overset{\sim t}{\boldsymbol{X}}_{ij_k}\right)^{\mathrm{T}} \overset{\sim t}{\boldsymbol{X}}_{ij_k}$ is decreasing. Given that $v^i_{t_{k+1}}$ decreases if $\overset{\sim t}{\boldsymbol{X}}_{ij_k}$ has a positive value, there must be $a_{ij_k}(t_{k+1}) \leq 0$ and $v^i_{t_{k+1}} = v_- < v^{j_k}_{t_{k+1}}$. The boundedness analysis of the velocity is finished.

As for the angular rate, we have:

$$\begin{aligned} \dot{\psi}^i_t = &-\frac{\sum_{k=1}^{L}\left[-\ k^2_{ij_k}\dot{\psi}^{j_k}_t \quad k^1_{ij_k}\ \right]\boldsymbol{\mathcal{T}}_{0i}\overset{\sim t}{\boldsymbol{X}}_{ij_k}}{v^i_t} \\ &-\sum_{k=1}^{L}\frac{k^2_{ij_k} v^{j_k}_t sin\left(\psi^{ij_k}_r\right) + sin\left(\psi^{ij_k}_r\right)a^{j_k}_t}{v^i_t} - \dot{\psi}^{j_k}_t \end{aligned} \tag{34}$$

Define $\dot{\psi}^i_t = \sum_{k=1}^{L}\theta^{ij_k}_t$ with

$$\begin{aligned} v^i_t\theta^{ij_k}_t &= -cos\left(\psi^{ij_k}_r\right)\left(k^1_{ij_k} y^e_{ij_k}(t) - k^2_{ij_k} x^e_{ij_k}(t)\dot{\psi}^{j_k}_t\right) \\ &= sin\left(\psi^{ij_k}_r\right)b_{j_k}(t) - cos\left(\psi^{ij_k}_r\right)a_{j_k}(t) + v^i_t\dot{\psi}^{j_k}_t \end{aligned} \tag{35}$$

We can obtain:

$$\left|v^i_t\theta^{ij_k}_t\right| \leq \left|\pi^{ij_k}_t\right| + \left|v^i_t\dot{\psi}^{j_k}_t\right| \leq 2k^2_{ij_k} v_m + \left|v^i_t\dot{\psi}^{j_k}_t\right| \tag{36}$$

Choosing $k^2_{ij_k} = \frac{|v^i_t|}{2v_m}\left(\omega_m - \left|\dot{\psi}^{j_k}_t\right|\right)$, we can obtain a group of α_{j_k} and β_{j_k}. Thus, Proposition 2 is proved and the input saturation is avoided. □

3.4. Communication Interference Resistance with Sensors

Based on Lemma 2, the nonlinear controller proposed in Section 3.3 might become invalid when agents encounter communication breaks as conditions of Proposition 1 cannot be met. Therefore, extra reference information should be provided, and sensors mounted on agents can complete the mission. In this paper, we discuss the requirements of the sensing graph and propose an estimator with only bearings measurement.

Firstly, we introduce the sensing graph $\mathcal{G}_s$, which is indicated as $(\mathcal{V}_s, \mathcal{E}_s)$, where $\mathcal{V}_s = \{v^i_s | i \in \mathcal{N}_a\}$ indicates the vertices, and $\mathcal{E}_s \subseteq \mathcal{V}_s \times \mathcal{V}_s$ represents the edges. Similar to $\mathcal{G}$, the adjacent matrix of $\mathcal{G}_s$ is defined as $\boldsymbol{A}_s = \left[a^{ij}_s\right]^N_{N}$, $a^{ij}_s > 0$ if agent i can sense information of agent j, otherwise $a_{ij} = 0$. Obviously, $\boldsymbol{A}_s$ is not necessary to be symmetric. Subsequently, the Laplacian matrix $\boldsymbol{\mathcal{L}}_s$ is indicated as $\boldsymbol{\mathcal{L}}_s = \left[l^{ij}_s\right]^N_{N}$, $l^{ij}_s = a^{ij}_s$ if $i \neq j$, otherwise $l^{ii}_s = -\sum a^{ij}_s$.

Stimulated by [22] restrictions should be put to $\boldsymbol{\mathcal{L}}_s$ with insufficient measured information, otherwise, the proposed controller in Proposition 1 will be invalid. The primary restriction is given with Theorem 2.

Theorem 2. *Multi-agent systems can keep stable with rank$\left(\boldsymbol{\mathcal{L}}\right) < N - N_l$ and rank$\left(\boldsymbol{\mathcal{L}} + \boldsymbol{\mathcal{L}}_s\right) = N - N_l$, if there exist communication interferences.*

Theorem 2 can be proved with Lemma 1 and various restrictions for different sensors. Next, we will discuss these restrictions required for stable formation.

As seen from the reference information processing in Section 2.3, distance information [8] is necessary for formation control, even in [1,21,25,29], velocity measurement is required for controller design. Therefore, bearings alone cannot provide sufficient information without information fusion. In this paper, we propose an estimator for relative positions with bearings only, and we give the model of bearings $\boldsymbol{b}^t_{ij}$ $\forall (i,j) \in \mathcal{E}_s$:

$$\boldsymbol{b}^t_{ij} = \frac{\boldsymbol{X}^t_{ij}}{\|\boldsymbol{X}^t_{ij}\|_2} \tag{37}$$

where $\boldsymbol{X}^t_{ij} = \boldsymbol{\mathcal{T}}_{0i}\left(\boldsymbol{X}^j_t - \boldsymbol{X}^i_t\right)$.

Then, take derivatives of $\boldsymbol{b}^t_{ij}$ and we can obtain:

$$D_1\left(\boldsymbol{b}^t_{ij}\right) = \frac{D_1\left(\boldsymbol{X}^t_{ij}\right)\|\boldsymbol{X}^t_{ij}\|^2_2 - \boldsymbol{X}^t_{ij}\left(\boldsymbol{X}^t_{ij}\right)^{\mathrm{T}} D_1\left(\boldsymbol{X}^t_{ij}\right)}{\|\boldsymbol{X}^t_{ij}\|^3_2} \tag{38}$$

Remark 3. *Equations (37) and (38) are both underdetermined with bearing $\boldsymbol{b}^t_{ij}$ only. If the relative positions can be obtained [8], then $\boldsymbol{b}^t_{ij}$ is useless. If the velocity can be sensed [21], then Equation (38) is determined and $D_1\left(\boldsymbol{X}^t_{ij}\right)$ can be obtained. The above analysis implies that the controller is valid with bearings information if Equations (37) and (38) can be solved, which means we must obtain $\boldsymbol{X}^t_{ij}$ with Equations (37) and (38), which can be considered as restrictions on $\boldsymbol{\mathcal{L}}_s$ in various situations.*

Situation 1. *Only bearings can be transmitted among agents or obtained by detecting, then we can obtain $\boldsymbol{X}^t_{ij}$ with Equations (37) and (38) if rank$\left(\boldsymbol{\mathcal{L}} + \boldsymbol{\mathcal{L}}_s\right) = N - N_l$ holds, where the number of positive elements must be greater than n for each row of $\boldsymbol{\mathcal{L}} + \boldsymbol{\mathcal{L}}_s$.*

Situation 2. *Extra reference can be transmitted among agents or obtained by detecting beside bearings, such as distance or velocity, then we can obtain $\boldsymbol{X}_{ij}^t$ with Equations (37) and (38) if $rank\left(\boldsymbol{\mathcal{L}}+\boldsymbol{\mathcal{L}}_s\right)=N-N_l$ holds.*

Situation 3. *Although extra reference can be transmitted among agents or obtained by detecting besides bearings, systems encounter communication breaks and some agents lose interaction with others, then we can obtain $\boldsymbol{X}_{ij}^t$ with Equations (37) and (38) if $rank\left(\boldsymbol{\mathcal{L}}+\boldsymbol{\mathcal{L}}_s\right)=N-N_l$ holds, and the number of positive elements of the corresponding rows of $\boldsymbol{\mathcal{L}}+\boldsymbol{\mathcal{L}}_s$ must be greater than n for agents without any interaction.*

According to the discussion, formation reconstruction might be necessary while encountering communication breaks. The autonomous system should adjust the motion parameters, thus agents without interaction could obtain sufficient measurement. With the above strategy, the estimator is proposed as:

$$\left(\boldsymbol{A}_s^i\otimes\boldsymbol{1}_{1\times 2n}\right)^{\mathrm{T}}\circ\boldsymbol{H}\left(\boldsymbol{X}_{ij}^t\right)=\boldsymbol{0} \tag{39}$$

where $\boldsymbol{A}_s^i=\left[a_s^{ij}\right]_1^N$ represents the adjacent vector of agent i, $\boldsymbol{H}\left(\boldsymbol{X}_{ij}^t\right)=\left[\boldsymbol{h}\left(\boldsymbol{X}_{ij}^t\right)\right]_{2nN}^1$, and $\boldsymbol{h}\left(\boldsymbol{X}_{ij}^t\right)$ is indicated as:

$$\boldsymbol{h}\left(\boldsymbol{X}_{ij}^t\right)=\begin{bmatrix}\boldsymbol{b}_{ij}^t\|\boldsymbol{X}_{ij}^t\|_2-\boldsymbol{X}_{ij}^t\\ D_1\left(\boldsymbol{b}_{ij}^t\right)-\frac{D_1\left(\boldsymbol{X}_{ij}^t\right)}{\|\boldsymbol{X}_{ij}^t\|_2}+\frac{\boldsymbol{X}_{ij}^t\left(\boldsymbol{X}_{ij}^t\right)^{\mathrm{T}}D_1\left(\boldsymbol{X}_{ij}^t\right)}{\|\boldsymbol{X}_{ij}^t\|_2^3}\end{bmatrix} \tag{40}$$

Considering the nonlinearity and measured deviation, (38) might have no closed-form analytic solution. Therefore, the nonlinear programming method is applied here, and the corresponding regulator is defined as:

$$\begin{aligned}&J=\|\left(\boldsymbol{A}_s^i\otimes\boldsymbol{1}_{1\times\mathrm{n}}\right)^{\mathrm{T}}\circ\boldsymbol{G}_{\boldsymbol{X}}\|_{\boldsymbol{Q}_s}\\&s.t.\\&\quad\left(\boldsymbol{A}_s^i\otimes\boldsymbol{1}_{1\times\mathrm{n}}\right)^{\mathrm{T}}\circ\boldsymbol{G}_{\boldsymbol{b}}=\boldsymbol{0}\end{aligned} \tag{41}$$

where $\boldsymbol{Q}_s$ is a symmetric positive matrix.

$$\begin{cases}\boldsymbol{G}_{\boldsymbol{b}}=\left[\boldsymbol{b}_{ij}^t\|\boldsymbol{X}_{ij}^t\|_2-\boldsymbol{X}_{ij}^t\right]_{nN}^1\\ \boldsymbol{G}_{\boldsymbol{X}}=\left[D_1\left(\boldsymbol{b}_{ij}^t\right)-\frac{D_1\left(\boldsymbol{X}_{ij}^t\right)}{\|\boldsymbol{X}_{ij}^t\|_2}+\frac{\boldsymbol{X}_{ij}^t\left(\boldsymbol{X}_{ij}^t\right)^{\mathrm{T}}D_1\left(\boldsymbol{X}_{ij}^t\right)}{\|\boldsymbol{X}_{ij}^t\|_2^3}\right]_{nN}^1\end{cases} \tag{42}$$

For agents that can keep communication with neighbors, the sensing information can be used for unbiased estimations. For agents without interaction (encountering communication breaks), sensing information is crucial for consensus keeping.

4. Numerical Simulation

4.1. Leader-Follower Model-Based Formation Control

Formation control with 8 agents is considered, each agent has a leader, and there is no communication break. The expected relative position is $[-69.2820, 40]$ or $[-69.2820, -40]$ in the reference frame, boundaries are $v_{max}=30$ m/s, $\omega_{max}=1$ rad/s. Initial states of agents are listed in Table 1.

As seen in Figure 2, all agents can form the expected formation and keep formation with the proposed controller. Fluctuations happen between steps 400 and 600 when the formation switch is performed, and agents conduct maneuvering among step 500 and step

550 with $\omega = 0.01\mathrm{rad/s}$. Compared with the traditional linear controller with constant parameters, results of which are shown in Figure 3, Figure 4, and Figure 5, the proposed controller can bound the velocity and angular rate according to Figures 6 and 7, and frequent shock is avoided.

Table 1. Initial states of test 1.

i	$X^i_{t_0}$ (m,m)	$q^i_{t_0}$ (m/s,rad)	$u^i_{t_0}$ (m/s^2,rad/s)
1	(28.2, 0.7)	(5, 0.6447)	(0, 0)
2	(49.6, 98.8)	(5, 0.3731)	(0, 0)
3	(73.8, 31.1)	(5, 0.7681)	(0, 0)
4	(60.0, 78.2)	(5, 1.2662)	(0, 0)
5	(11.1, 57.9)	(5, 0.5935)	(0, 0)
6	(87.0, 69.0)	(5, 0.8136)	(0, 0)
7	(24.3, 34.3)	(5, 0.1486)	(0, 0)
8	(54.5, 6.7)	(5, 1.4280)	(0, 0)

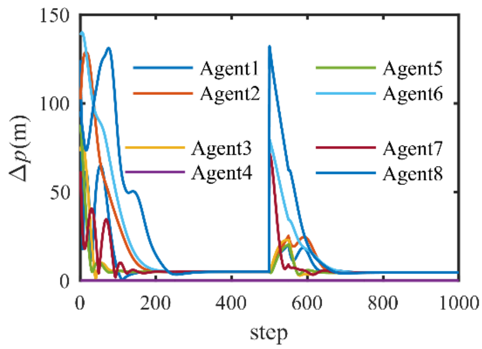

Figure 2. Position errors with the proposed controller.

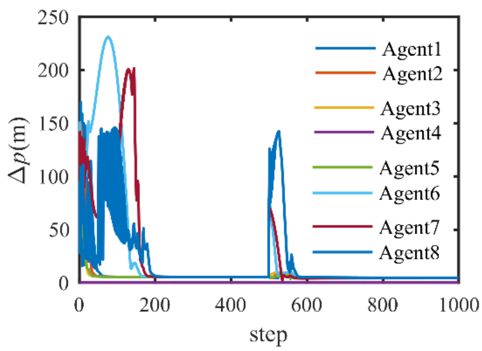

Figure 3. Position errors with linear controller.

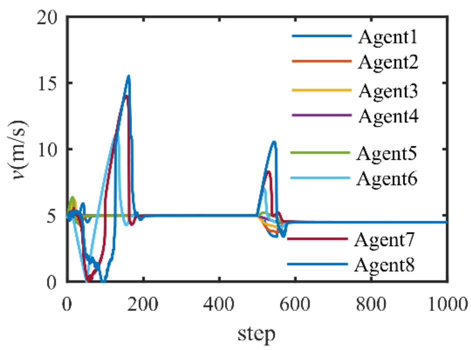

Figure 4. Velocity control result with linear controller.

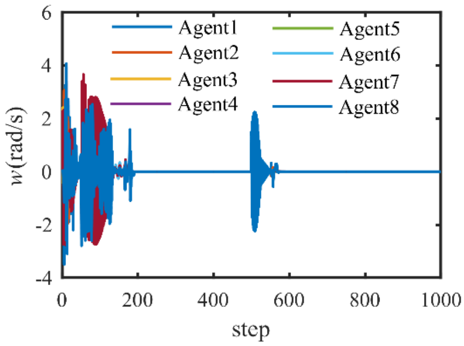

Figure 5. Angular rate control result with linear controller.

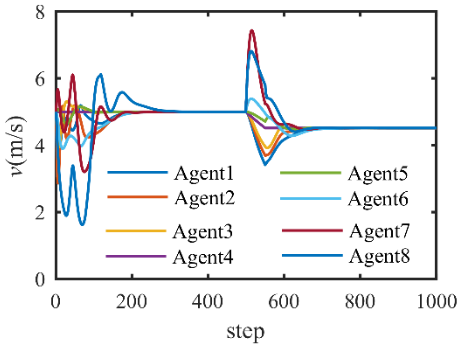

Figure 6. Velocity control with the proposed controller.

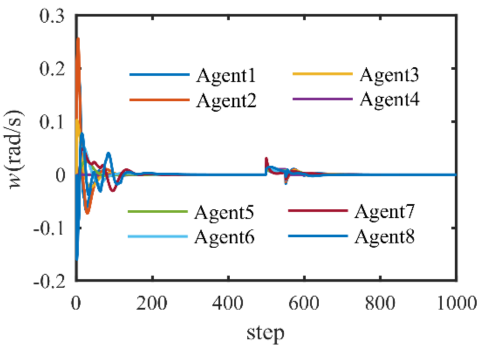

Figure 7. Angular rate control with the proposed controller.

4.2. Formation Control with Communication Break

Boundaries remain unchanged, agent 2 encountered communication breaks between steps 500 and 550, and distance and velocity information can be sensed. Initial states of agents are listed in Table 2.

Table 2. Initial states of test 2.

i	$X^i_{t_0}$ (m,m)	$q^i_{t_0}$ (m/s,rad)	$u^i_{t_0}$ (m/s^2,rad/s)
1	(30.3, 81.7)	(5, 2.4997)	(0, 0)
2	(−31.2, −67.5)	(5, 2.0965)	(0, 0)
3	(−58.1, −47.2)	(5, 1.4426)	(0, 0)
4	(−33.5, 28.8)	(5, 5.8818)	(0, 0)
5	(−104.3, 11.8)	(5, 4.2926)	(0, 0)
6	(−38.9, 55.0)	(5, 6.0451)	(0, 0)
7	(−42.8, 0.38)	(5, 2.7519)	(0, 0)
8	(−46.8, −34.1)	(5, 5.9083)	(0, 0)

Since at step 0 the formation is not complete, each agent should have reasonable reference information before step 200. The maneuvering time is between 700 and 710, thus the velocity fluctuation exists in Figure 8. Agent 2 encountered a communication break between steps 500 and 550; therefore, the errors increase at step 500 for agent 2. Figures 8 and 9 show that the boundaries of velocity and angular rate are satisfied. Figure 10 shows that communication breaks and maneuvering affect the formation to a certain extent, but the formation is kept ultimately. Considering that agent i can obtain relatively sufficient reference information from other nearby agents with sensors while encountering a communication break, agent i can keep pace with others to some extent. Figure 11 displays the track of the formation in this test.

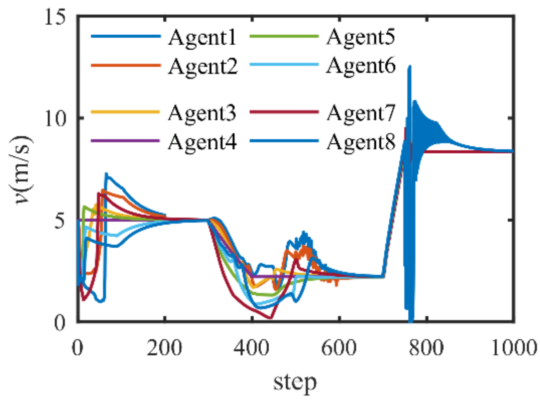

Figure 8. Velocity (test 2).

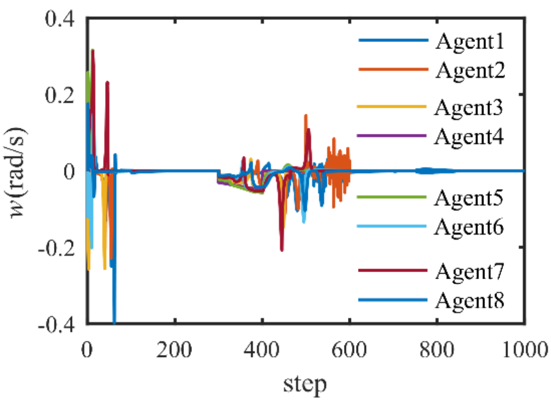

Figure 9. Angular rate (test 2).

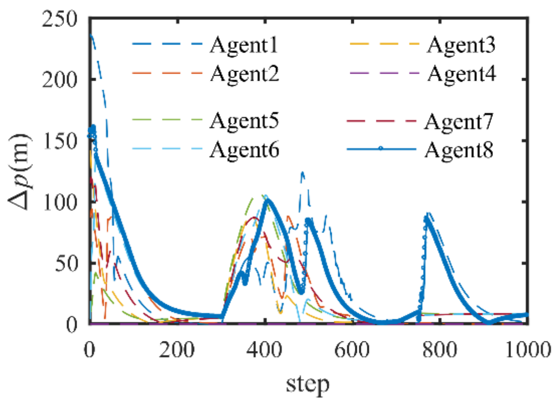

Figure 10. Position errors (test 2).

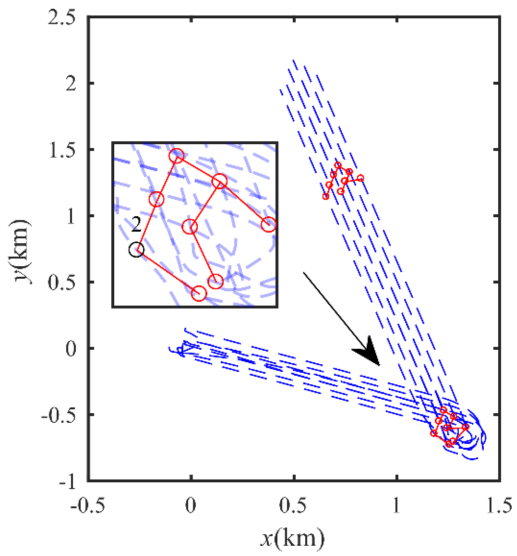

Figure 11. Track with communication breaks (test 2).

4.3. Formation Keep with Bearings Only

Based on the second simulation, the worse condition is considered, agent i could not obtain distance and velocity referred information, which means agent i must realize formation keeping with only bearings information. In this part, we consider that agent 8 lost all communication from step 500 to 800, and it can detect the relative bearing of agent 2 and agent 6, the maneuvering starts at step 300, and finishes at step 400. The turning rate is changing based on $\omega = \left(0.01 - \frac{t-100}{5000}\right)\mathrm{rad/s}$.

The duration of the communication interruption is longer compared with test two, and no distance and velocity information can be sensed. Therefore, the positional error of agent 8 is larger, which is shown with the bold line in Figure 12. However, fortunately, the positional error of agent 8 is decreasing slowly, although there exists only bearings information, the formation is kept to some extent, which is shown in Figure 13. Due to communication breaks, control of velocity and angular rate are not so smooth, which can be found in Figures 14 and 15, but the boundaries are satisfied in general. As can be seen from Figure 14, the turning maneuvering impacts the formation a lot, the time-varying angular rate will cause shock, and agents behind will suffer more effects. In this paper, no devices damage is considered, but the formation control results of persistent communication interruption show that agents without communication can be capable of roughly tracking refereed agents, although the tracking is not ideal.

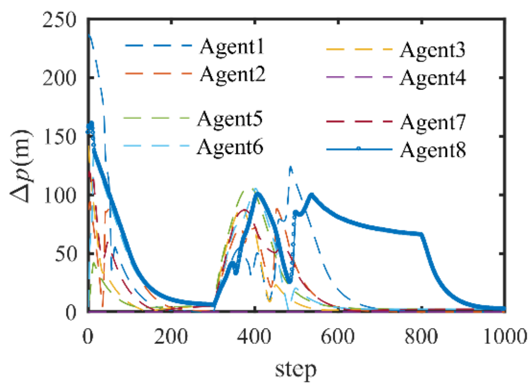

Figure 12. Position errors (test 3).

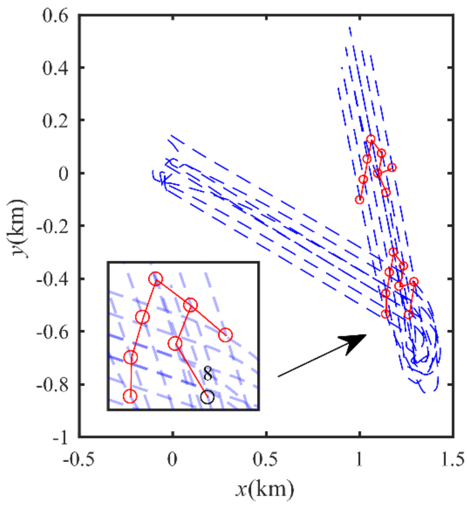

Figure 13. Track with bearings only (test 3).

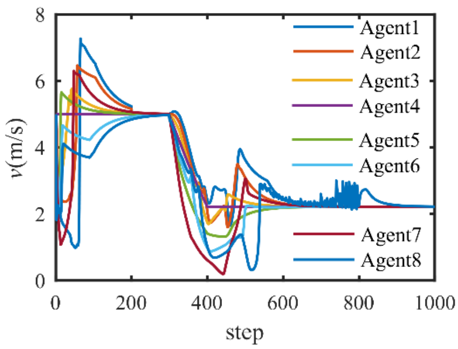

Figure 14. Velocity (test 3).

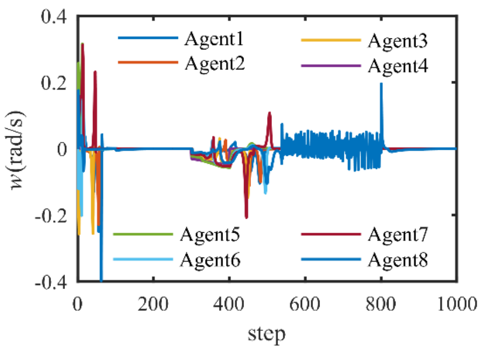

Figure 15. Angular rate (test 3).

5. Conclusions

This paper surveys stable formation control for multi-agent systems with communication breaks due to link failure and communication barriers. Considering the nonlinearity caused by maneuvers during formation acquisition, a novel nonlinear controller is proposed based on the CA algorithm. Using the Lyapunov function method and the distance-based function, an adaptive rule of parameters of the controller is put forward for anti-saturation control. In addition, the conditions of reference information are analyzed. Based on the sensing graph, the feasibility of formation keeping with bearings only is considered, and a dynamic programming regulator is proposed for unknown reference (relative positions and velocity) estimation. The proposed regulator provides auxiliary reference information for the controller, and the formation is kept encountering communication breaks. To addresses collisions among agents, the artificial potential field method is utilized for the law revision.

Mathematical and numerical analysis shows that the controller is feasible and stable. Future research will focus on precise and more efficient control with bearings information and formation switch in environments with obstacles.

Author Contributions: Conceptualization, Z.X.; Funding acquisition, J.X.; Investigation, Z.L.; Methodology, Z.X. and Y.L.; Software, Z.X. All authors have read and agreed to the published version of the manuscript.

Funding: This research was funded by National Natural Science Foundation of China grant number [51679247].

Informed Consent Statement: Not applicable.

Conflicts of Interest: The authors declare no conflict of interest.

References

1. Gwihan, K.; Minh, H.T.; Hyo-Sung, A. Bearing-only control of directed cycle formations: Almost global convergence and hardware implementation. *Int. J. Robust Nonlinear Control* **2020**, *30*, 4789–4804. [CrossRef]
2. Arijit, S.; Soumya, R.S.; Mangal, K. Nonlinear formation control strategies for agents without relative measurements under heterogeneous networks. *Int. J. Robust Nonlinear Control* **2017**, *28*, 1653–1671. [CrossRef]
3. Xiwang, D.; Chao, S.; Guoqiang, H. Time-varying output formation control for linear multi-agent systems with switching topologies. *Int. J. Robust Nonlinear Control* **2016**, *26*, 3558–3579. [CrossRef]
4. Daifeng, Z.; Haibin, D. Switching topology approach for UAV formation based on binary-tree network. *J. Frankl. Inst.* **2019**, *356*, 835–859. [CrossRef]
5. Iman, S.; Khashayar, K. Actuator fault accommodation strategy for a team of multi-agent systems subject to switching topology. *Automatica* **2015**, *62*, 200–207. [CrossRef]
6. JunHao, R.; XiaoFeng, Z. Containment Control of Multi-Agent Systems with Stochastic Multiplicative Noises. *J. Syst. Sci. Complex.* **2021**. [CrossRef]
7. Changduo, L.; Mingfeng, G.; Zhiwei, L.; Guang, L.; Feng, L. Predefined-time formation tracking control of networked marine surface vehicles. *Control. Eng. Pract.* **2021**, *107*, 104682. [CrossRef]
8. Farhad, M.; Farzad, H.; Mahdi, B.; Marcio, D.Q. Finite-Time Rigidity-Based Formation Maneuvering of Multiagent Systems Using Distributed Finite-Time Velocity Estimators. *IEEE Trans. Cybern.* **2019**, *49*, 4473–4484. [CrossRef]
9. Bong, S.P.; Sung, J.Y. Connectivity-maintaining and collision-avoiding performance function approach for robust leader–follower formation control of multiple uncertain underactuated surface vessels. *Automatica* **2021**, *127*, 109501. [CrossRef]
10. Hamed, R.; Farzaneh, A. Motion synchronization in unmanned aircrafts formation control with communication delays. *Commun. Nonlinear Sci. Numer. Simul.* **2013**, *18*, 744–756. [CrossRef]
11. Mohammad, A.D.; Mohammad, B.M. Communication free leader–follower formation control of unmanned aircraft systems. *Robot. Auton. Syst.* **2016**, *80*, 69–75. [CrossRef]
12. Tagir, Z.M.; Rustem, A.M. Consensus-based cooperative control of parallel fixed-wing UAV formations via adaptive backstepping. *Aerosp. Sci. Technol.* **2021**, *109*, 106416. [CrossRef]
13. Yusuf, K.; Kamesh, S.; Nicholas, R.G.; Atilla, D.; Frank, L. Distributed backstepping based control of multiple UAV formation flight subject to time delays. *IET Control. Theory Appl.* **2020**, *14*, 1628–1638. [CrossRef]
14. Do, K.D. Bounded and inverse optimal formation stabilization of second-order agents. *Automatica* **2021**, *123*, 109367. [CrossRef]
15. ShiKai, S.; Yu, P.; Chenglong, H.; Yu, D. Efficient path planning for UAV formation via comprehensively improved particle swarm optimization. *ISA Trans.* **2020**, *97*, 415–430. [CrossRef]
16. AliNoormohammadi, A.; Mohammad, B.M.; Atena, S. Control of leader-follower formation and path planning of mobile robots using asexual reproduction optimization (ARO). *Appl. Soft Comput.* **2014**, *14*, 563–576. [CrossRef]
17. Ahmed, T.H.; Anthony, J.M.; Sidney, N.G.; Mohamad, I.; Shahram, Y.; Camille, A.R. Solving multi-UAV dynamic encirclement via model predictive control. *IEEE Trans. Control. Syst. Technol.* **2015**, *23*, 2251–2265. [CrossRef]
18. Ahmed, T.H.; Sidney, N.G.; Shahram, Y. Unmanned Aerial Vehicles Formation Using Learning Based Model Predictive Control. *Asian J. Control* **2018**, *20*, 1014–1026. [CrossRef]
19. Qishao, W.; Zhisheng, D.; Yuezu, L.; Qingyun, W.; Guanrong, C. Linear quadratic optimal consensus of discrete-time multi-agent systems with optimal steady state: A distributed model predictive control approach. *Automatica* **2021**, *127*, 109505. [CrossRef]
20. Qishao, W.; Zhisheng, D.; Jingyao, W.; Guanrong, C. LQ Synchronization of Discrete-Time Multi-Agent Systems: A Distributed Optimization Approach. *IEEE Trans. Autom. Control* **2019**, *64*, 5183–5190. [CrossRef]
21. Choi, H.L.; Brunet, L.; How, J.P. Consensus-Based Decentralized Auctions for Robust Task Allocation. *IEEE Trans. Robot.* **2009**, *25*, 912–926. [CrossRef]
22. Zhiqi, T.; Rita, C.; Tarek, H.; Carlos, S. Formation control of a leader–follower structure in three dimensional space using bearing measurements. *Automatica* **2021**, *128*, 109567. [CrossRef]

23. Guanghui, W.; Zhisheng, D.; Wei, R.; Guanrong, C. Distributed consensus of multi-agent systems with general linear node dynamics and intermittent communications. *Int. J. Robust Nonlinear Control* **2014**, *24*, 2438–2457. [CrossRef]
24. Xiaowen, F.; Jing, P.; Haixiang, W.; Xiaoguang, G. A formation maintenance and reconstruction method of UAV swarm based on distributed control. *Aerosp. Sci. Technol.* **2020**, *104*, 105981. [CrossRef]
25. Michalska, H.; Mayne, D.Q. Robust receding horizon control of constrained nonlinear systems. *IEEE Trans. Autom. Control* **1993**, *38*, 1623–1633. [CrossRef]
26. Sun, Z.; Dai, L.; Liu, K.; Xia, Y.; Johansson, K.H. Robust MPC for tracking constrained unicycle robots with additive disturbances. *Automatica* **2018**, *90*, 172–184. [CrossRef]
27. Zongyu, Z.; Lin, T. Distributed robust finite-time nonlinear consensus protocols for multi-agent systems. *Int. J. Syst. Sci.* **2016**, *47*, 1366–1375. [CrossRef]
28. Chenfeng, H.; Xianku, Z.; Guoqing, Z. Adaptive neural finite-time formation control for multiple underactuated vessels with actuator faults. *Ocean. Eng.* **2021**, *222*, 108556. [CrossRef]
29. Florent, L.B.; Tarek, H.; Robert, M.; Claude, S. Observers for Position Estimation Using Bearing and Biased Velocity Information. In *Sensing and Control for Autonomous Vehicles*; Lecture Notes in Control and Information Sciences; Springer: Cham, Switzerland, 2017; Volume 474, pp. 3–23. [CrossRef]